Journal of Atmospheric and Solar-Terrestrial Physics ▮ (▮▮▮▮) ▮▮▮–▮▮▮

Contents lists available at ScienceDirect

Journal of Atmospheric and Solar-Terrestrial Physics

journal homepage: www.elsevier.com/locate/jastp

Focusing of HF radio-waves by ionospheric ducts

G.M. Milikh [a], A. Vartanyan [a,*], K. Papadopoulos [a], M. Parrot [b]

[a] Department of Physics and Astronomy, University of Maryland, College Park, Maryland, USA
[b] Laboratoire de Physique et Chimie de l'Environnement et de l'Espace, CRNS, Orleans, France

ARTICLE INFO

Article history:
Received 29 October 2010
Received in revised form
25 February 2011
Accepted 28 February 2011

Keywords:
Radio wave focusing
Ionospheric ducts
Ionospheric heating
Satellite observations

ABSTRACT

This paper presents the first direct observations of HF focusing induced by natural and artificial ionospheric ducts along with a simple theoretical model. The experiments were conducted by injecting HF radio-waves using the Ionospheric Research Instrument of the High Frequency Active Auroral Research Program located in Gakona, Alaska and detecting them with instruments on the overflying French micro-satellite DEMETER. The latter observed a multiple frequency band structure, which is characteristic of a strong HF signal exceeding the detector's saturation level. Analysis of the O^+ density measured by DEMETER along its orbit shows that the strong radio signal coincides with the presence of a "negative" duct in the ionosphere. "Negative" refers to the presence of a plasma density depletion with the peak depletion located near the center of the duct. Such ducts induce changes in the index of refraction leading to the focusing of HF waves in a manner equivalent to a "thick" plasma lens. Examination of the data along with a simple plasma lens model indicates the presence of focal node(s) in the vicinity of the overflying satellite. Two examples, one corresponding to focusing by a natural duct and one by an artificial one are presented.

Published by Elsevier Ltd.

1. Introduction

The possibility of focusing HF radio-waves in the ionosphere by natural or artificial plasma lenses has been the subject of theoretical studies and speculation starting more than 40 years ago (Bliokh and Bryukovetskiy, 1969; Gurevich et al., 1976). In addition, more recently Kosch et al. (2007) explained their optical observations by modeling HF radio beam self-focusing due to formation of a "depleted plasma filament", while Leyser and Nordblad (2009) numerically simulated HF focusing of the O-mode wave with regard to heating experiments at HAARP. In the case of Gurevich et al. (1976), theoretical models indicated that changes in the index of refraction of the ionospheric plasma driven by HF-heating can form thin (a few tens of km) plasma lenses that can focus the radio-waves to satellite altitudes. The analysis indicated that the focal length of such "thin" lenses was two or more thousand km above the heating region, thus making their experimental detection difficult. In fact there has yet to be an experimental confirmation of the process.

Similar focusing can be accomplished by "negative" ionospheric ducts. By negative ducts we refer to plasma density depletion elongated along the geomagnetic field lines. The natural negative ducts are often known as troughs. Such ducts can be either natural or artificially created by the HF-heating effect. Ducts can have plasma density gradients sufficient to cause refraction of HF waves. Since "negative" ducts are elongated field aligned regions of plasma depletion, HF waves propagating into a negative duct experience a positive change of the refractive index, thus focusing the waves towards the center of the duct. This is illustrated by Fig. 1, which shows a schematic of HF focusing by ionospheric ducts. Outside the lens the focused beam propagates inside the duct, reflects from the duct's walls, and as a result produces focal nodes. Ionospheric ducts are much thicker than the "thin" lens mentioned earlier, and can thus be considered as "thick" plasma lenses. In this paper we present the first experimental evidence of ionospheric HF focusing by a "thick" plasma lens along with a simple model of this process.

The experiments discussed below were conducted by injecting HF radio-waves using the Ionospheric Research Instrument (IRI) of the High Frequency Active Auroral Research Program (HAARP) located in Gakona, Alaska and detected by instruments on the overflying French micro-satellite DEMETER.

2. Experimental observations

DEMETER flies on a 670 km circular polar orbit and overflies HAARP twice a day, once at nighttime between 6:00 and 7:00 UT, and another at daytime between 20:00 and 21:00 UT. Its onboard

* Corresponding author. Tel.: +1 240 246 4659.
E-mail addresses: milikh@astro.umd.edu (G.M. Milikh), aramvar@umd.edu (A. Vartanyan), dennis.papadopoulos@gmail.com (K. Papadopoulos), Michel.Parrot@cnrs-orleans.fr (M. Parrot).

1364-6826/$ - see front matter Published by Elsevier Ltd.
doi:10.1016/j.jastp.2011.02.022

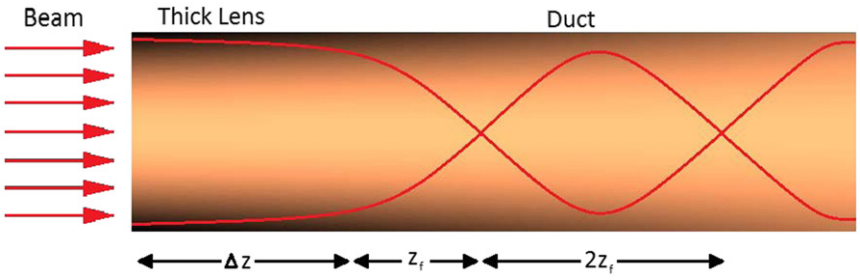

Fig. 1. Schematic of HF wave focusing by ionospheric ducts. Areas of darker or lighter colors represent higher or lower plasma density, respectively. The wavy lines show the path of radio rays after they enter the lens/duct system and also demonstrate the formation of multiple "nodes". (For interpretation of the references to color in this figure legend, the reader is referred to the web version of this article.)

diagnostic instruments are often used to detect effects driven by the interaction of HF waves injected by the IRI with the ionospheric plasma. Optimum time for diagnosing such experiments is when the satellite flies in close proximity to HAARP, i.e. distances closer than 100 km from the HAARP magnetic zenith. Such coincidences occur approximately four times a week (twice at daytime and twice at nighttime).

A set of experiments, in which the HAARP IRI operating at power 3.6 MW and 84.1 dBW ERP injected O-mode radio-waves at a frequency of 2.8 MHz along the HAARP magnetic zenith (MZ), were monitored by DEMETER overflying close to the HAARP MZ. MZ heating and 2.8 MHz frequency were chosen to closely match the f_oF_2 peak, because previous experiments indicated that they maximize the probability for duct formation. Two DEMETER diagnostic instruments were used for this particular experiment. The first instrument was the ICE (Electric Field Instrument), which monitors HF signals in the frequency range from a few kHz to 3.3 MHz (Berthelier et al., 2006a). The second instrument was the IAP (Plasma Analyzer Instrument), which measures the ion temperature and composition (Berthelier et al., 2006b). Our particular experiment focused on density measurements of O^+ ions – the most abundant ions in the F-region. In addition, the local ionospheric conditions were monitored by the HAARP ionosonde.

The HF spectrogram observed by the ICE on 02/12/10 at 6:29–6:33 UT is shown at the bottom of Fig. 2. In this experiment the closest distance of DEMETER from the MZ was 38 km. The observed spectral "line" at 2.8 MHz that extends between 40.3° and 65° latitude – over 2800 km – is generated by radio emission stimulated by the interaction of the injected HF with the F-region plasma, rather than by the direct "free space" IRI signal. We will return to this point later in the paper. We should mention here that the maximum detection frequency of ICE is 3.3 MHz. This restriction prevents detection of daytime duct effects since frequencies above 4 MHz are required to match the daytime f_oF_2 peak.

We now focus our attention on the strong multiple-frequency band structure observed between 6:30:40 and 6:30:50 UT. Such a structure is indicative of the ICE receiving a strong HF signal exceeding its saturation level, which at 2.8 MHz is approximately 10 mV/m. Analysis of the O^+ density measured by DEMETER along its orbit (see the top of Fig. 2) shows that the strong signal detected by ICE almost coincides with the presence of a "negative" duct in the ionosphere. Plasma quasi-neutrality in the ionosphere requires that the electron density exhibit a similar profile. It is well known that depletion in electron density leads to positive perturbations in the index of refraction. Thus incident HF waves propagating into this plasma channel with an inverted density profile will be focused towards the center of the duct.

Fig. 3 shows another example of duct focusing observed on 10/21/09. DEMETER's closest approach to HAARP's MZ was 27 km. The ionosphere was quiet with the F_2 layer peak at 220 km and $f_oF_2=2.05$ MHz. An important difference between this case and the previous one involves the issue of natural vs. artificial ducts and will be addressed in Section 4. The ICE HF spectrogram in Fig. 3 (bottom) shows a band at about 06:28:15 in the entire frequency range of the instrument. Fig. 3 (top) shows the O^+ density measured by DEMETER during this experiment. This is also indicative of the presence of a negative duct, although not as distinct as in the 02/12/10 experiment.

3. Theoretical model

A simple theoretical model can be formulated by considering a plane wave with (angular) frequency ω propagating along the field aligned density depletion shown in Fig. 1. The index of refraction at F-region heights is $\eta=\sqrt{1-\omega_{pe}^2/\omega^2}$, where $\omega_{pe}=\sqrt{ne^2/\varepsilon_0 m}$ is the electron plasma frequency, and n is the electron density. In the presence of the density duct the index of refraction is perturbed due to the change in the electron density. Assuming a density perturbation Δn with $\Delta n/n \ll 1$ the perturbed index of refraction $\Delta\eta$ can be expressed as

$$\Delta\eta=\frac{\partial\eta}{\partial n}\Delta n=-\frac{1}{2}\frac{\omega_{pe}^2/\omega^2}{\sqrt{1-\omega_{pe}^2/\omega^2}}\frac{\Delta n(z,\rho)}{n(z)}. \quad (1)$$

Here $n(z)$ is the ambient electron density. Following Gurevich et al. (1976), the electric field at distance z_1 from the lower boundary of a duct and radius ρ is given by

$$E=Ae^{i\psi_o}\frac{\omega}{2\pi ic}\int\frac{\exp\left[i\Delta\varphi(z_1,\rho)+i(\omega/c)r\right]}{r}\rho\,d\rho. \quad (2)$$

Here A is the amplitude of the wave at the lower boundary of the duct and $r=\sqrt{z_1^2+\rho^2}$. The perturbed phase of the wave at a distance z_1 along the duct is given by

$$\Delta\varphi=\frac{\omega}{c}\int_o^{z_1}\Delta\eta\,dz. \quad (3)$$

In the absence of the phase perturbation $\Delta\varphi=0$ and $|E|=A$. Expanding $\Delta\varphi$ in powers of ρ^2

$$\Delta\varphi=\Delta\varphi_0+\rho^2\Delta\varphi_1+\rho^4\Delta\varphi_2+\ldots$$

and taking into account that $\rho/z_1\ll 1$ i.e. that the duct has a limited transverse size, we find that

$$r=z_1\left(1+\frac{\rho^2}{2z_1^2}+\cdots\right).$$

Focusing occurs when the phase in the exponent of Eq. (2) approaches zero (Gurevich et al., 1976). Thus, to second order

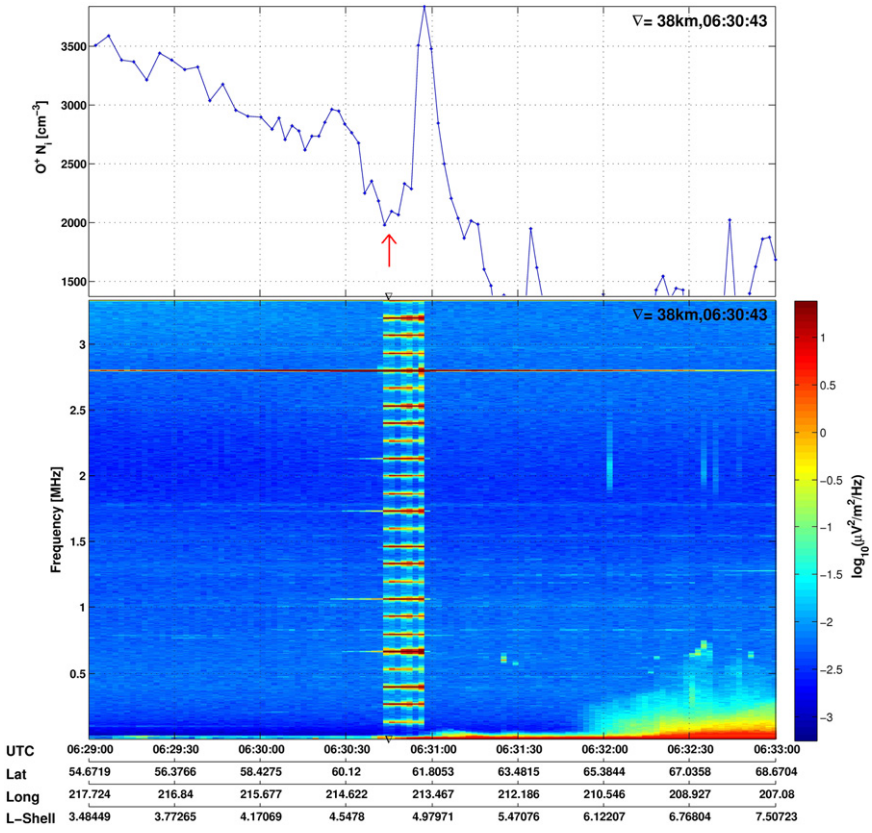

Fig. 2. Shown on the top is the density of positive ions of atomic oxygen observed by the IAP instrument onboard DEMETER made on 02/12/10. Shown on the bottom is the high frequency electric field power spectrum observed by the ICE instrument onboard DEMETER made on 02/12/10. The horizontal trace at 2.8 MHz corresponds to the frequency radiated by IRI. The *x*-axes show the time of the observations, along with the corresponding satellite latitude, longitude and L-shell. The arrow points to the minimum of the relevant negative duct.

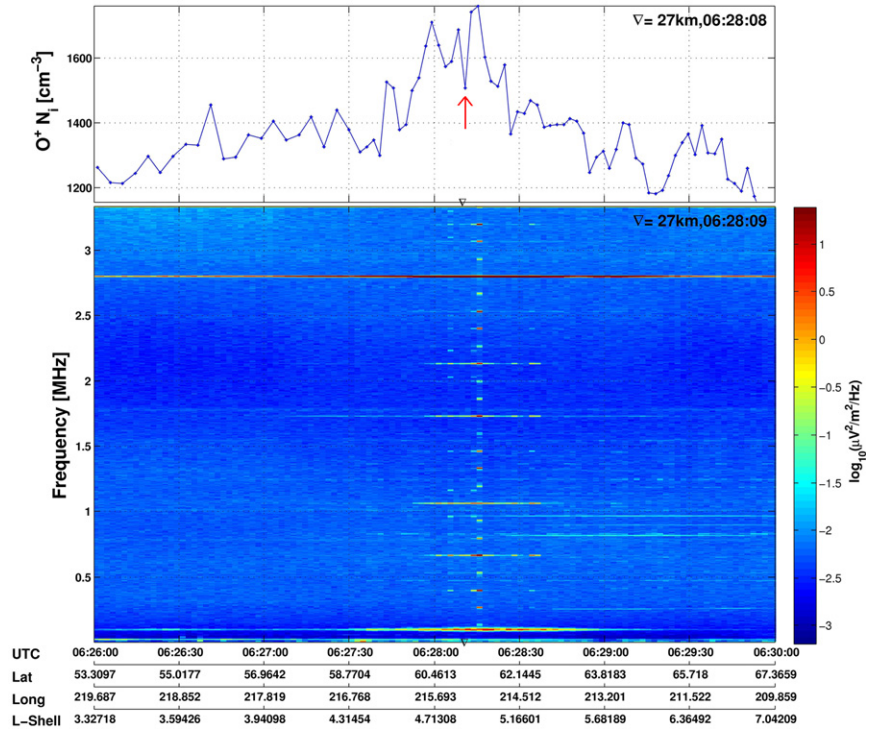

Fig. 3. Same as Fig. 2 but observed on 10/21/09.

Please cite this article as: Milikh, G.M., et al., Focusing of HF radio-waves by ionospheric ducts. Journal of Atmospheric and Solar-Terrestrial Physics (2011), doi:10.1016/j.jastp.2011.02.022

ARTICLE IN PRESS

in ρ/z_1, the focal distance z_f satisfies the equation

$$\Delta\varphi_1+\frac{\omega}{2z_fc}=\frac{\omega}{2c}\int_o^{z_f}\frac{\omega_{pe}^2/\omega^2}{\sqrt{1-\omega_{pe}^2/\omega^2}}\frac{1}{n}\frac{\partial\Delta n}{\partial\rho^2}\,dz-\frac{\omega}{2c}\frac{1}{z_f}=0. \tag{4}$$

Solving Eq. (4) for z_f we find that

$$z_f=\left\{\int_o^{z_f}\frac{\omega_{pe}^2/\omega^2}{\sqrt{1-\omega_{pe}^2/\omega^2}}\frac{1}{n}\frac{\partial\Delta n}{\partial\rho^2}\,dz\right\}^{-1}. \tag{5}$$

From this point forward we will take the above expression and evaluate it using certain assumptions that are tailored to each of our described experiments. We first focus our attention to the experiment performed on 2/12/2010 and assume for simplicity that the duct obeys cylindrical symmetry about the magnetic field, i.e. ρ_0=constant. In addition we note that the combination of ω_{pe}^2/ω^2 and $1/n$ is a constant, and assume that the electron density above the F_2 peak can be modeled as a decaying exponential: $\omega_{pe}^2/{\omega_0}^2=n/n_0=\exp(-z/H)$, where ω_0 and n_0 are the plasma frequency and density at the F_2 peak, respectively, and H is to be chosen in such a way that $n(z_{SAT})$ gives the ambient electron density measured by the DEMETER satellite. After these simplifications Eq. (5) becomes

$$\frac{1}{z_f}=\frac{\omega_0^2}{\omega^2}\frac{1}{{\rho_0}^2}\int_o^{z_f}\frac{\Delta n(z)}{n_0}\frac{dz}{\sqrt{1-(\omega_0^2/\omega^2)e^{-z/H}}}. \tag{6}$$

The functional form of Δn remains to be specified, and to do so we use EISCAT observations of a quiet-time ionospheric trough (Voiculescu et al., 2010). In this paper the electron density of an ionospheric trough was measured at EISCAT at different altitudes, and it was shown that the density depletion (Δn) decreases with altitude. Assuming that the decrease is exponential, the functional form of Δn becomes $\Delta n=\Delta n_0\exp(-\alpha(z/H))$, where $\Delta n_0=\Delta n_{SAT}\exp(\alpha(z_{SAT}/H))$ is the density depletion measured at the F_2 peak, Δn_{SAT} is measured by the DEMETER satellite, and α is the decay constant to be quoted later. Finally we introduce normalized coordinates $\tilde{z}_f=z_f/H$ and $\xi=z/H$ and thus Eq. (6) becomes

$$\frac{1}{\tilde{z}_f}=\frac{\omega_0^2}{\omega^2}\frac{H^2}{{\rho_0}^2}\frac{\Delta n_0}{n_0}\int_o^{\tilde{z}_f}\frac{e^{-\alpha\xi}\,d\xi}{\sqrt{1-(\omega_0^2/\omega^2)e^{-\xi}}}. \tag{7}$$

This equation can be readily solved numerically as soon as the experiment and duct parameters are specified.

We now shift our attention to the focusing observations made on 10/21/2009. This case differs from the previous case since in this case the duct was of artificial origin, which was caused by the plasma outflow moving along the geomagnetic field line from the HF-heated region located near the F_2 peak of the ionosphere (Milikh et al., 2010). Such plasma is magnetized is contained within the duct of almost constant radius and density perturbation (ρ_0=constant and $\Delta n=\Delta n_0$=constant). Moreover the term in the denominator in Eq. (7) deviates from unity by less than 10% for this specific case, and thus can be safely replaced by unity. After these assumptions the expression for the focal length becomes

$$\frac{1}{\tilde{z}_f}=\frac{\omega_0^2}{\omega^2}\frac{H^2}{{\rho_0}^2}\frac{\Delta n_0}{n_0}\int_o^{\tilde{z}_f}d\xi,$$

or solving for the focal length we get

$$z_f=\rho_0\frac{\omega}{\omega_0}\sqrt{\frac{n_0}{\Delta n(z_{SAT})}}. \tag{8}$$

From Eq. (2) the amplification of the electric field amplitude caused by focusing is given by

$$\left|\frac{E}{A}\right|=\frac{\omega}{2\pi c}\frac{\rho_0^2}{z_f}, \tag{9}$$

and it is valid for either of the experiments.

Note that Eqs. (6) and (8) are similar to focusing and magnification by optical lenses. The focal distance is proportional to the lens aperture and inversely proportional to the optical density of the lens material. The lens material (refractive index) and frequency control the magnification coefficient.

4. Analysis of experimental observations

We proceed here to use the observations in conjunction with the theoretical model to examine three key physics issues: consistency of expected focal length and magnification with observations, evidence for natural or artificial origin of ducts, and implications of the 10–20 kHz broadening of the observed 2.8 MHz signal.

4.1. Focal length and magnification – theory vs. observations

Referring first to the 02/12/2010 experiment we note that according to Fig. 2, at DEMETER's altitude the horizontal size of the duct is about 170 km, i.e. $\rho_0=85\pm15$ km (see Appendix for details on uncertainty), the relative depletion of the plasma density inside the duct is $\Delta n_{SAT}=1000\pm150\,cm^{-3}$, while the unperturbed density immediately south of the duct is about $n(z_{SAT})=2950\pm50\,cm^{-3}$. The value of z_{SAT} is simply 670–300=370 km, while H was found to be about 110 km, and the F_2 peak density n_0 can be computed using the value of $\omega_0=2\pi(2.55\,MHz)$ from HAARP's ionosonde. Notice that the above value of the characteristic plasma density scale (H=110 km) is in good agreement with the IRI ionospheric model's value of 100 km (Bilitza et al., 2001).

Based on the density data in Voiculescu et al. (2010), the decay constant was estimated to be $\alpha=.6\pm.1$ (see Appendix). On the basis of these estimates, corresponding uncertainty ranges, and Eq. (7) we can estimate the focal length of the focusing duct as about 430 ± 75 km. Thus the duct whose lower boundary is located around the F_2 peak at 300 km provides optimal focusing at about 730 ± 75 km. From Eq. (9) we find that a wave having frequency f=2.8 MHz is magnified by 150 ± 45 times at the focal point. We can estimate the magnification at DEMETER's altitude by assuming the focused beam has a conical shape, thereby decreasing the magnification by a factor $((z_f-d)/z_f)^2$, where d is the distance between the focal point and DEMETER's orbit. The result is a magnification of about 110 ± 50 at DEMETER's altitude. Our estimates show that during its pass on 02/12/10, DEMETER was located within the focal point uncertainty range of the "lens" formed by the negative duct in the ionosphere. Therefore its antenna received a strongly amplified signal. Furthermore, considering that the power density detected by ICE outside of the duct was 25 $(\mu V/m)^2/Hz$, and considering that the half bandwidth of the signal is about 12 kHz (which will be discussed below), we find that the strongest signal outside of the perturbed region was about 0.5 mV/m. Since calibration tests prior to the flight gave a 10 mV/m saturation level at 2.8 MHz, the observations of Fig. 2 require a focusing of at least by 20, which is within the uncertainty range of the magnification and is thus consistent with the observations.

Referring next to the 10/21/09 case we note that the top of Fig. 3 shows the clear detection of an artificial duct, which was detected by DEMETER's plasma analyzer instrument (IAP) and

Please cite this article as: Milikh, G.M., et al., Focusing of HF radio-waves by ionospheric ducts. Journal of Atmospheric and Solar-Terrestrial Physics (2011), doi:10.1016/j.jastp.2011.02.022

Langmuir probe (ISL), where the latter measures the electron temperature and density. While only observations from the IAP are shown in Fig. 3, both instruments reveal simultaneous increase of the ion and electron density and temperature when overflying the MZ of HAARP. This infallibly shows formation of the artificial duct; see also the discussion in Section 4.2.

Moreover, at 06:28:10 the bottom of Fig. 3 shows a strong band in the spectrogram, which coincides with a local negative duct (marked by an arrow) having peak density depletion of $\Delta n = 150 \pm 20\ \mathrm{cm}^{-3}$ and radius $\rho_0 = 17 \pm 3$ km (see Appendix for details of uncertainties). Following Eq. (8) the focal length of the focusing duct is about 430 km from the F_2 peak, producing 6.5 ± 2.5 times magnification at the focal point of this lens (see Eq. (9) with $f = 2.8$ MHz). We can estimate the magnification at DEMETER's altitude by our previous method of assuming a conical shape for the focused beam. The result is a magnification of about 5 ± 2 at DEMETER's altitude.

At this point we should mention that a duct is a much more efficient focusing lens than a thin perturbed layer proposed in (Bliokh and Bryukovetskiy, 1969; Gurevich et al., 1976) since according to Eq. (6) above the focusing distance for a thin lens is $z_f \simeq \left((\omega_0^2/\omega^2)(\Delta z/\rho_0^2)(\Delta n/n_0)\right)^{-1}$. Thus for typical parameters of the HF-heated region in the ionosphere $\Delta z = 10$ km, $\Delta n/n \le 0.1$, $\rho_0 > 50$ km the focusing distance $z_f > 2500$ km. Such focusing can hardly be detected by a lower orbit satellite.

4.2. Natural vs. artificial ducts

A key question raised by the data is whether the focusing is due to a preexisting natural duct or due to a duct created by the HF heating. In answering this question we are guided by the two instruments on board DEMETER and by the HAARP digisonde, which operates on two different modes. The first mode produces regular ionograms while the second mode produces Doppler sky maps by measuring a number of directional ionograms caused by plasma irregularities.

Our previous experience indicates that formation of artificial ducts is associated with upward ion flow in the vicinity of the MZ. As a result Doppler sky maps show a cluster of reflections formed around the magnetic zenith with negative Doppler (Milikh et al., 2010). During the 02/12/10 experiment while the sky maps did not show any such negative Doppler shifts near the MZ they indicated the presence of a large number of irregularities, moving towards North West with average velocity 763 ± 44 m/s and upward with the velocity 67 ± 1 m/s. This is consistent with natural duct formation.

On the other hand during the 10/21/09 experiment the ionosonde showed a regular F_2 peak well matched to the heating frequency, as well as absence of sporadic E-layer, conditions resulting in efficient HF-heating. Unfortunately sky maps were not available during this experiment. Both instruments on board DEMETER showed a distinct positive duct which indicates its artificial origin. This duct had a fine structure. In fact, the arrow in Fig. 3 shows a negative duct located on top of the artificial positive duct. We thus surmise that this focusing was caused by an artificial duct.

4.3. Significance of HF line broadening

In examining the 2.8 MHz spectral region observed in both experiments (Figs. 2 and 3) we note that while the IRI signal was of high purity (bandwidth of few Hz) the signal observed over the entire 2800 km region shows a half-width of 12 kHz at a 3 dB level when measured away from the strongly perturbed region (trace 1 in Fig. 4). In the perturbed region the signal is much broader, its half-width reaches 35 kHz (trace 2 in Fig. 4). We

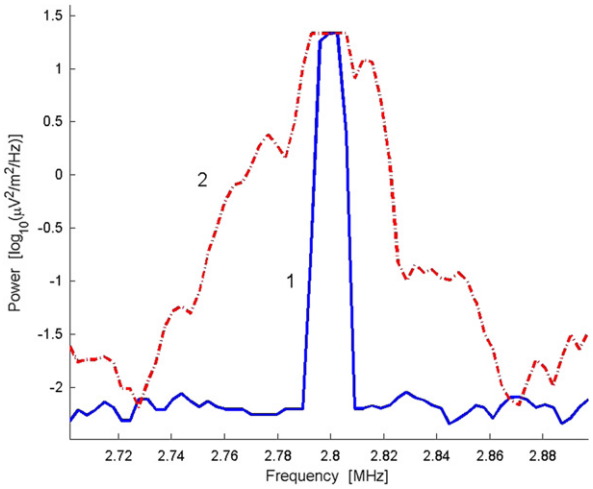

Fig. 4. Power density of the signals detected by DEMETER as a function of frequency. Traces 1 and 2 correspond to the measurements made at 6:31:16 and 6:30:52, respectively.

believe that this is evidence that the HF emission detected by DEMETER does not represent a direct signal sent by the IRI but corresponds to Stimulated Electromagnetic Emission (SEE) generated by the HF-heating induced turbulence. It is also worth noting that even if the discussed effect was caused by the interaction of the direct IRI beam with the satellite, the interactive region will be 250 km. Thus the interaction time will be 33 s, more than twice the observed time seen in the experiment made on 02/12/10. Moreover, previous experiments have been conducted during times when the ionosphere was highly perturbed. In these cases the IRI beam would propagate presumably with little absorption and hit DEMETER's antenna and create a multi-frequency band structure as before, and yet not once was such an effect observed during experiments we have conducted in the past few years.

SEE has often been detected on the ground below the heated spot and has been the subject of numerous theoretical and experimental studies (Thidé et al., 1983; Stubbe and Kopka, 1990; Stubbe et al., 1994; Norin et al., 2009). The peak amplitude E_d detected by DEMETER was much weaker than the free space fields E_{fs}. In fact, the E_d/E_{fs} ratio was in the range of $(0.5–4.6) \times 10^{-2}$. Note that the HF signals were detected by DEMETER over a long time 1.4–5.5 min, i.e. along 580–2100 km of the DEMETER orbit. This corresponds to a uniformly radiating source located in the F-region, while the well directed HAARP antenna limits the receiving distance to 300–400 km along the orbit. In the future we plan to make observations of SEE from the ground while simultaneously making observations from the above using DEMETER's ICE and IAP. We expect that comparison of the ground vs. space measured spectra can yield important information on heater induced turbulence.

5. Conclusion

This paper presented what we believe to be the first direct observations of HF focusing induced by natural and artificial ionospheric ducts along with a simple theoretical model. The experiments were conducted by injecting HF radio-waves using the Ionospheric Research Instrument of the High Frequency Active Auroral Research Program located in Gakona, Alaska and detecting them with instruments on the overflying French micro-satellite DEMETER. Two specific experiments were presented, where observations using DEMETER's ICE instrument showed the presence of multiple frequency band structures that are

Please cite this article as: Milikh, G.M., et al., Focusing of HF radio-waves by ionospheric ducts. Journal of Atmospheric and Solar-Terrestrial Physics (2011), doi:10.1016/j.jastp.2011.02.022

characteristic of a strong HF signal exceeding the detector's saturation level. It was also noted that the strong radio signal coincided with the presence of a "negative" duct in the ionosphere. A simple theoretical model was presented which showed that the presence of a negative duct can lead to focusing at satellite altitudes with enough magnification to cause instrument saturation, thus showing consistency with our observations. The observation of the HF signal over a range of more than 1000 km with a bandwidth of 10–20 kHz is evidence of detection of SEE waves rather than direct HF IRI radiation. The reported phenomenon can be used in HF communications, and in diagnostics of the upper ionosphere.

Acknowledgments

The work was supported by DARPA via a subcontract N684228 with BAE Systems, and by the ONR Grant NAVY.N0017302C60 and ONR MURI Grant N00014010789. The authors thank J.J. Berthelier for the use of his data.

Appendix A

A.1. Estimation of duct width and density depletion uncertainties

In order to estimate the duct properties and corresponding uncertainties, a systematic method for fitting an appropriate function to the duct was needed; the following describes this systematic method. For the 2/12/10 observation, the ion density data points that comprise the negative duct were isolated, and MATLAB's curve fitting toolbox (cftool) was used to fit a parabola of the form $ax\hat{}2+bx+c$. An appropriate cutoff for the parabola was then chosen for the estimation of the width and density depletion of the duct. That cutoff was chosen to be the ambient ion density immediately south of the duct (solid black line in Fig. A1) while the corresponding uncertainty was estimated by observing the density fluctuations immediately south of the duct (dashed black lines in Fig. A1). The cftool gave the best values for a, b, c and their corresponding 90% confidence bounds, which along with the ambient density of $2950 \pm 50\ \mathrm{cm}^{-3}$ were used to estimate the duct radius $\rho_0 = 85 \pm 15$ km, and density depletion $\Delta n_{SAT} = 1000 \pm 150\ \mathrm{cm}^{-3}$. Fig. A1 shows the resulting duct fitting and corresponding uncertainty bounds, with analogous solid and dashed lines for the former and latter.

For the 10/21/2009 observation a slightly different approach had to be taken since the duct we wish to fit has only three data points that comprise it. A parabola fitting of only those three points would obviously give no confidence bounds. Instead, two parabola fittings were performed, and the range of duct parameters from these two fits were used to define an uncertainty (dashed red lines in Fig. A2). An intermediate fit representing the "actual" fit (solid red line in Fig. A2) was constructed by averaging the fitting parameters from the first two parabola fits. Similar to before, a cutoff for the parabola was chosen by averaging the points surrounding the negative duct (solid black line in Fig. A2), while the corresponding uncertainty was estimated from the standard deviation (dashed lines in Fig. A2), resulting in an "ambient" density of $1650 \pm 50\ \mathrm{cm}^{-3}$. The parabola fitting gave a peak density depletion of $\Delta n = 150 \pm 20\ \mathrm{cm}^{-3}$ and duct radius $\rho_0 = 17 \pm 3$ km.

A.2. Uncertainty in the α parameter

The estimation of the α parameter is achieved through the use of EISCAT observations of a quiet-time ionospheric trough from Voiculescu et al. (2010). On page 17 of the paper, ionospheric trough density curves can be seen for altitudes 264, 306, 345, and 435 km. Recalling that we need the density depletion dependence on altitude above the F_2 peak and noting that 306 km is almost exactly at the F_2 peak, we see that only the data points for the three higher altitudes will be relevant. In fact, the middle of those three can be disregarded for the sake of simplicity since in that case the calculation of α simply amounts to solving $\Delta n/\Delta n_0 = \exp(-\alpha(\Delta z/110))$, where Δn_0 and Δn are the density depletions at altitudes 306 and 435 km, respectively, while $\Delta z = 435-306 \approx 130$ km. Moreover, the EISCAT paper provides density observations for four different hours and thus α can be estimated four times. An estimate of α for the four different times in chronological order is .55, .4, .6, and .8. The average of the four estimates gives $\alpha \approx .6$ and was the value of α quoted earlier. The uncertainty is found using a standard result from error

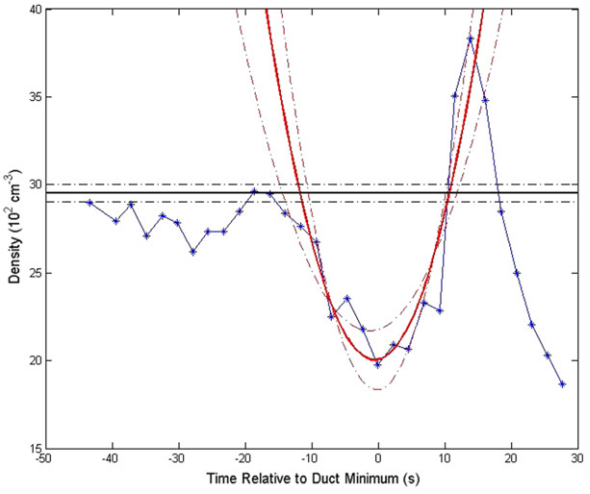

Fig. A1. Parabola fitting of negative duct observed on 2/12/10. The solid red parabolic curve attempts to hug the points of the negative duct; the dashed parabolas illustrate the confidence bounds on the fit. Analogously the ambient density and uncertainty range can be seen in black. (For interpretation of the references to color in this figure legend, the reader is referred to the web version of this article.)

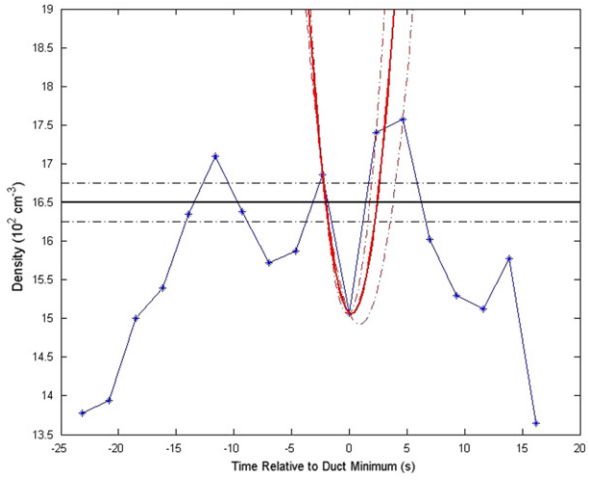

Fig. A2. Same as Fig. A1, except for the observations made on 10/21/09. (For interpretation of the references to color in this figure legend, the reader is referred to the web version of this article.)

ARTICLE IN PRESS

propagation theory, namely that $\sigma_{avg}=\sigma/\mathrm{sqrt}(N)$, where N is the number of points used (4). The final result for α is $.6 \pm .1$.

References

Berthelier, J.J., Godefroy, M., Leblanc, F., et al., 2006a. ICE, the electric field experiment on DEMETER. Planet. Space Sci. 54, 456.

Berthelier, J.J., Godefroy, M., Leblanc, F., et al., 2006b. IAP, the thermal plasma analyzer on DEMETER. Planet. Space Sci. 54, 487.

Bilitza, D., Papitashvili, N., King, J., 2001. IRI related data and model services at NSSDC. Adv. Space Res. 27, 133–141.

Bliokh, P.V., Bryukovetskiy, A.S., 1969. Focusing of radio waves by an artificially created ionospheric lens. Geomagn. Aeron. 9, 443–446.

Gurevich, A.V., Milikh, G.M., Shluger, I.S., 1976. Nonlinear thermal focusing of radio waves in the lower ionosphere. Geomagn. Aeron. 16, 613–619.

Kosch, M.J., Pedersen, T., Mishin, E., et al., 2007. Temporal evolution of pump beam self-focusing at the high-frequency active auroral research program. J. Geophys. Res. 112, A08304. doi:10.1029/2007JA012264.

Leyser, T.B., Nordblad, E., 2009. Self-focused radio frequency L wave pumping of localized upper hybrid oscillations in high-latitude ionospheric plasma. Geophys. Res. Lett. 36, L24105. doi:10.1029/2009GL041438.

Milikh, G.M., Mishin, E., Galkin, I., Vartanyan, A., Roth, C., Reinisch, B., 2010. In situ detection of HF-induced ducts in the topside ionosphere. Geophys. Res. Lett. 37, L18102. doi:10.1029/2010GL044636.

Norin, L., Leyser, T.B., Nordblad, E., et al., 2009. Unprecedentedly strong and narrow electromagnetic emissions stimulated by high-frequency radio waves in the ionosphere. Phys. Rev. Lett. 102, 065003.

Stubbe, P., Kopka, H., 1990. Stimulated electromagnetic emission in a magnetized plasma: a new symmetric spectral feature. Phys. Rev. Lett. 65 (2), 183–185.

Stubbe, P., Stocker, A.J., Honary, F., Robinson, T.R., Jones, T.B., 1994. Stimulated electromagnetic emissions (SEE) and anomalous HF wave absorption near electron gyroharmonics. J. Geophys. Res. 99 (A4), 6233–6246.

Thidé, B., Derblom, H., Hedberg, Å., et al., 1983. Observations of stimulated electromagnetic emissions in ionospheric heating experiments. Radio Sci. 18 (6), 851–859.

Voiculescu, M., Nygrén, T., Aikio, A., Kuula, R., 2010. An olden but golden EISCAT observation of a quiet-time ionospheric trough. J. Geophys. Res. 115, A10315. doi:10.1029/2010JA015557.

Please cite this article as: Milikh, G.M., et al., Focusing of HF radio-waves by ionospheric ducts. Journal of Atmospheric and Solar-Terrestrial Physics (2011), doi:10.1016/j.jastp.2011.02.022